Journal of Sound and Vibration 329 (2010) 485–496

Contents lists available at ScienceDirect

Journal of Sound and Vibration

journal homepage: www.elsevier.com/locate/jsvi

Free vibration analysis of continuous rectangular plates

M. Huang [a], X.Q. Ma [b,*], T. Sakiyama [c], H. Matsuda [c], C. Morita [c]

[a] North China Electric Power University, Beijing 102206, PR China
[b] Hebei University of Technology, Tianjing 300130, PR China
[c] Department of Structural Engineering, Nagasaki University, Nagasaki 852, Japan

ARTICLE INFO

Article history:
Received 26 December 2007
Received in revised form
12 June 2009
Accepted 31 August 2009
Handling Editor: L.G. Tham
Available online 29 October 2009

ABSTRACT

Vibration characteristics of rectangular plates continuous over full range line supports or partial line supports have been studied by using a discrete method. Concentrated loads with Heaviside unit functions and Dirac delta functions are used to simulate the line supports. The fundamental differential equations are established for the bending problem of the continuous plate. By transforming these differential equations into integral equations and using the trapezoidal rule of the approximate numerical integration, the solution of these equations is obtained. Green function which is the solution of deflection of the bending problem of plate is used to obtain the characteristic equation of the free vibration. The effects of the line support, the variable thickness and aspect ratio on the frequencies and mode shapes are considered. By comparing the numerical results obtained by the present method with those previously published, the efficiency and accuracy of the present method are investigated.

1. Introduction

Plates continuous over intermediate supports have been used extensively in civil, aircraft and marine structures. The vibration analysis of these plates is important for avoiding the resonance. According to the length of the supports, the plates with straight line supports are divided into two kinds, one is plates continuous over full line supports and another is plates continuous over partial line supports. For the plates with full line supports, the dynamic characteristics have been investigated by using different methods. An approximate analytical method was used by Takahashi and Chishaki to determine the vibration characteristics of plates continuous over full line supports in one direction [1] and in two directions [2]. Numerical results were given for simply supported plates. The receptance method was used by Azimi et al. [3] to analyze the free vibration of thin rectangular plates continuous over full line supports parallel to two simply supported edges and with other two opposite edges clamped or simply supported. Numerical results were presented for four-equal-span, four-unequal-span, three-equal-span and three-unequal-span plates. The other methods, such as the Rayleigh–Ritz method [4,5], the finite strip method [6], the finite layer approach [7] and the Lévy method [8] were also used. Lin and his cooperators [9,10] analyzed free vibration of a finite row of continuous skin-stringer panels and column-supported cooling towers. Mead and Yaman [11,12] studied the harmonic response of rectangular sandwich plates with multiple stiffening and beams on multiple linear supports. For the plates with partial line supports, the dynamic study of these plates is rather limited. Xiang et al. [13] investigated the vibration behaviors of continuous rectangular plates by using the discrete singular convolution algorithm. Some results for the rectangular plates continuous over partial internal line supports were also presented. All of the above papers are limited to the plates with uniform thickness.

* Corresponding author. Tel.: +86 2227593773; fax: +86 2260435279.
E-mail address: xiuqin_m@hebut.edu.cn (X.Q. Ma).

0022-460X/$ - see front matter © 2009 Published by Elsevier Ltd.
doi:10.1016/j.jsv.2009.08.036

In this paper, a discrete method [14] is expanded for analyzing the free vibration of rectangular plates with variable thickness and continuous over full range line supports or partial line supports, which are simulated by concentrated loads with Heaviside unit functions and Dirac delta functions. No prior assumption of shape of deflection used in the finite element method is employed in this method. Basing the first shear deformation theory, the fundamental differential equations of a plate involving Heaviside unit function and Dirac delta function are established. By transforming these equations into integral equations and using numerical integration, the solutions are obtained at the discrete points. Furthermore, by choosing the integral area in an appointed order, the solutions are only related to the unknown quantities on the boundary and that makes the number of unknown quantities decrease greatly. The solution for deflection is chosen as the Green function and used to obtain the characteristic equation of the free vibration. In this paper, the efficiency and accuracy of the present method for the continuous rectangular plates are investigated, and some numerical results and mode shapes are presented for the plate with variable thickness and continuous over full range and partial line supports.

2. Fundamental differential equations

Consider a rectangular plate of length a, width b, density ρ. An xyz coordinate system is used in the present study with its $x-y$ plane contained in the middle plane of the rectangular plate, the z-axis perpendicular to the middle plane of the plate and the origin at one of the corners of the plate, as shown in Fig. 1.

In this paper, the concentrated loads with Heaviside unit functions and Dirac delta functions are used to simulate the line supports. The deflection w, the rotations θ_x, θ_y, the shearing forces Q_x, Q_y, the twisting moment M_{xy} and the bending moments M_x, M_y are used as variables.

As given in Ref. [15], the fundamental differential equations of the plate having a concentrated load $\overline{P}$ at a point (x_q, y_r), the line support $\overline{R}_c(x,y)$ parallel to x-direction within the domain of $x_{c1} \le x \le x_{c2}$ and the line support $\overline{R}_d(x,y)$ parallel to y-direction within the domain of $y_{d1} \le y \le y_{d2}$ are as follows:

$$\frac{\partial Q_x}{\partial x} + \frac{\partial Q_y}{\partial y} + \overline{P}\delta(x-x_q)\delta(y-y_r) + \sum_{c=0}^{m} \overline{R}_c H[(x_{c2}-x_c)(x_c-x_{c1})]\delta(x-x_c)\delta(y-y_d) + \sum_{d=0}^{n} \overline{R}_d H[(y_{d2}-y_d)(y_d-y_{d1})]\delta(x-x_c)\delta(y-y_d) = 0, \tag{1a}$$

$$\frac{\partial M_{xy}}{\partial x} + \frac{\partial M_y}{\partial y} - Q_y = 0, \tag{1b}$$

$$\frac{\partial M_x}{\partial x} + \frac{\partial M_{xy}}{\partial y} - Q_x = 0, \tag{1c}$$

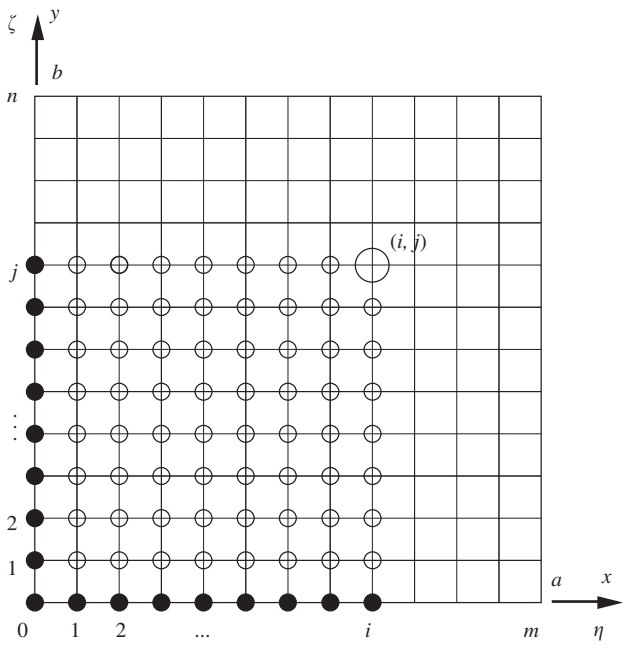

Fig. 1. Discrete points on a rectangular plate.

$$\frac{\partial\theta_x}{\partial x}+v\frac{\partial\theta_y}{\partial y}=\frac{M_x}{D}, \tag{1d}$$

$$\frac{\partial\theta_y}{\partial y}+v\frac{\partial\theta_x}{\partial x}=\frac{M_y}{D}, \tag{1e}$$

$$\frac{\partial\theta_x}{\partial y}+\frac{\partial\theta_y}{\partial x}=\frac{2}{(1-v)}\frac{M_{xy}}{D}, \tag{1f}$$

$$\frac{\partial w}{\partial x}+\theta_x=\frac{Q_x}{Gt_s}, \tag{1g}$$

$$\frac{\partial w}{\partial y}+\theta_y=\frac{Q_y}{Gt_s}, \tag{1h}$$

where $D=Eh^3/(12(1-v^2))$ is the bending rigidity; E and G are modulus and shear modulus of elasticity, respectively; v is Poisson's ratio; h is the thickness of plate; $t_s=h/1.2$; $\delta(x-x_q)$, $\delta(y-y_r)$, $\delta(x-x_c)$ and $\delta(y-y_d)$ are Dirac delta functions; $H[(x_{c2}-x_c)(x_c-x_{c1})]$ and $H[(y_{d2}-y_d)(y_d-y_{d1})]$ are Heaviside unit functions.

By introducing the non-dimensional expressions,

$$[X_1,X_2]=\frac{a^2}{D_0(1-v^2)}[Q_y,Q_x],\quad [X_3,X_4,X_5]=\frac{a}{D_0(1-v^2)}[M_{xy},M_y,M_x],\quad [X_6,X_7,X_8]=[\theta_y,\theta_x,w/a],$$

where $D_0=Eh_0^3/(12(1-v^2))$ is the standard bending rigidity; h_0 is the standard thickness of the plate, Eqs. (1a)–(1h) can be expressed as the following simple equation system:

$$\begin{aligned}\sum_{s=1}^{8}\left\{F_{1ts}\frac{\partial X_s}{\partial\zeta}+F_{2ts}\frac{\partial X_s}{\partial\eta}+F_{3ts}X_s\right\}+P\delta(\eta-\eta_q)\delta(\zeta-\zeta_r)\delta_{1t}+\sum_{c=0}^{m}R_cH[(\eta_{c2}-\eta_c)(\eta_c-\eta_{c1})]\delta(\eta-\eta_c)\delta(\zeta-\zeta_d)\delta_{1t}\\+\sum_{d=0}^{n}R_dH[(\zeta_{d2}-\zeta)(\zeta-\zeta_{d1})]\delta(\eta-\eta_c)\delta(\zeta-\zeta_d)\delta_{1t}\\=0\quad(t=1\sim8),\end{aligned} \tag{2}$$

where $P=\overline{P}a/(D_0(1-v^2))$; $R_c=\overline{R}_ca/(D_0(1-v^2))$; $R_d=\overline{R}_da/(D_0(1-v^2))$; $\delta(\eta-\eta_q)$, $\delta(\zeta-\zeta_r)$, $\delta(\eta-\eta_c)$ and $\delta(\zeta-\zeta_d)$ are Dirac delta functions; $H[(\eta_{c2}-\eta_c)(\eta_c-\eta_{c1})]$ and $H[(\zeta_{d2}-\zeta_d)(\zeta_d-\zeta_{d1})]$ are Heaviside unit functions; F_{1ts}, F_{2ts} and F_{3ts} are given in Appendix A.

3. Discrete Green function

As given in Ref. [14], by dividing a rectangular plate vertically into m equal-length parts and horizontally into n equal-length parts as shown in Fig. 1, the plate can be considered as a group of discrete points which are the intersections of the $(m+1)$-vertical and $(n+1)$-horizontal dividing lines. To describe the present method conveniently, the rectangular area, $0\le\eta\le\eta_i$, $0\le\zeta\le\zeta_j$, corresponding to the arbitrary intersection (i,j) as shown in Fig. 1 is denoted as the area $[i,j]$, the intersection (i,j) denoted by ○ is called the main point of the area $[i,j]$, the intersections denoted by ◦ are called the inner dependent points of the area, and the intersections denoted by • are called the boundary dependent points of the area.

By integrating Eq. (2) over the area $[i,j]$ and applying the trapezoidal integration rule, the simultaneous equation for the unknown quantities $X_{sij}=X_s(\eta_i,\zeta_j)$ at the main point (i,j) of the area $[i,j]$ is obtained as follows:

$$\begin{aligned}\sum_{s=1}^{8}\left\{F_{1ts}\sum_{k=0}^{i}\beta_{ik}(X_{skj}-X_{sk0})+F_{2ts}\sum_{l=0}^{j}\beta_{jl}(X_{sil}-X_{s0l})\quad+F_{3ts}\sum_{k=0}^{i}\sum_{l=0}^{j}\beta_{ik}\beta_{jl}X_{skl}\right\}\\+\left(Pu_{iq}u_{jr}+\sum_{c=0}^{m}R_cH_cu_{ic}u_{jd}\quad+\sum_{d=0}^{n}R_dH_du_{ic}u_{jd}\right)\delta_{1t}=0\quad(t=1\sim8),\end{aligned} \tag{3}$$

where $\beta_{ik}=\alpha_{ik}/m;\beta_{jl}=\alpha_{jl}/n$; $\alpha_{ik}=1-(\delta_{0k}+\delta_{ik})/2$; $\alpha_{jl}=1-(\delta_{0l}+\delta_{jl})/2$; $i=1\sim m$; $j=1\sim n$; $u_{iq}=u(\eta_i-\eta_q)$; $u_{jr}=u(\zeta_j-\zeta_r)$; $u_{ic}=u(\eta_i-\eta_c)$; $u_{jd}=u(\zeta_j-\zeta_d)$; $H_c=H[(\eta_{c2}-\eta_c)(\eta_c-\eta_{c1})]$, $H_d=H[(\zeta_{d2}-\zeta_d)(\zeta_d-\zeta_{d1})]$.

By retaining the quantities at main point (i,j) on the left hand side of the equation, putting other quantities on the right hand side and using the matrix transition, the solution X_{pij} of the above Eq. (3) is obtained as follows:

$$\begin{aligned}X_{pij}=\sum_{t=1}^{8}\left\{\sum_{k=0}^{i}\beta_{ik}A_{pt}[X_{tk0}-X_{tkj}(1-\delta_{ik})]+\sum_{l=0}^{j}\beta_{jl}B_{pt}[X_{t0l}-X_{til}(1-\delta_{jl})]+\sum_{k=0}^{i}\sum_{l=0}^{j}\beta_{ik}\beta_{jl}C_{ptkl}X_{tkl}(1-\delta_{ik}\delta_{jl})\right\}\\-A_{p1}\left(Pu_{iq}u_{jr}+\sum_{c=0}^{m}R_cH_cu_{ic}u_{jd}+\sum_{d=0}^{n}R_dH_du_{ic}u_{jd}\right),\end{aligned} \tag{4}$$

where $p=1\sim8$, A_{pt}, B_{pt} and C_{ptkl} are given in Appendix A.

In Eq. (4), the quantity X_{pij} is not only related to the quantities X_{tk0} and X_{t0l} at the boundary dependent points but also the quantities X_{tkj}, X_{til} and X_{tkl} at the inner dependent points. The maximal number of the unknown quantities is $6(m-1)(n-1)+(4m+4n+1)$. In order to reduce the unknown quantities, the area $[i,j]$ is spread according to the regular order as $[1,1],[1,2],\ldots,[1,n],[2,1],[2,2],\ldots,[2,n],\ldots,[m,1],[m,2],\ldots,[m,n]$. With the spread of the area according to the above mentioned order, the quantities X_{tkj}, X_{til} and X_{tkl} at the inner dependent points can be eliminated by substituting the obtained results into the corresponding terms of the right hand side of Eq. (4). By repeating this process, the quantity X_{pij} at the main point is only related to the quantities X_{rk0} ($r=1,3,4,6,7,8$) and X_{s0l} ($s=2,3,5,6,7,8$) at the boundary dependent points. The maximal number of the unknown quantities is reduced to $(4m+4n+1)$. It can be noted the number of the unknown quantities of the present method is fewer than that of the finite element method for the same divisional number $m(\geq 3)$ and $n(\geq 3)$. Based on the above consideration, Eq. (4) is rewritten as follows:

$$X_{pij}=\sum_{d=1}^{6}\left\{\sum_{f=0}^{i}\overline{a}_{pijfd}X_{rf0}+\sum_{g=0}^{j}\overline{b}_{pijgd}X_{s0g}\right\}+\overline{q}_{pij}P+\sum_{c=0}^{m}\overline{q}_{1pijcd}R_c+\sum_{d=0}^{n}\overline{q}_{2pijcd}R_d, \tag{5}$$

where $\overline{a}_{pijfd}$, $\overline{b}_{pijgd}$, $\overline{q}_{pij}$, $\overline{q}_{1pijcd}$ and $\overline{q}_{2pijcd}$ are given in Appendix B.

Eq. (5) gives the discrete solution of the fundamental differential Eq. (2) of the bending problem of a plate with a concentrated load and line supports, and the discrete Green function is chosen as $X_{8ij}a^2/[PD_0(1-\nu^2)]$, that is $w(x_0,y_0,x,y)/\overline{P}$.

4. Characteristic equation

By applying the Green function $w(x_0,y_0,x,y)/\overline{P}$ which is the displacement at a point (x_0,y_0) of a plate with a concentrated load $\overline{P}$ at a point (x,y), the displacement amplitude $\hat{w}(x_0,y_0)$ at a point (x_0,y_0) of the rectangular plate with line supports during the free vibration is given as follows:

$$\hat{w}(x_0,y_0)=\int_0^a\int_0^b\rho h\omega^2\hat{w}(x,y)[w(x_0,y_0,x,y)/\overline{P}]\,\mathrm{d}x\,\mathrm{d}y \tag{6}$$

where ρ is the mass density of the plate material.

By using the trapezoidal integration rule and the following non-dimensional expressions,

$$\lambda^4=\frac{\rho_0h_0\omega^2a^4}{D_0(1-\nu^2)},\quad k=1/(\mu\lambda^4),\quad H(\eta,\zeta)=\frac{\rho(x,y)}{\rho_0}\frac{h(x,y)}{h_0},$$
$$W(\eta,\zeta)=\frac{\hat{w}(x,y)}{a},\quad G(\eta_0,\zeta_0,\eta,\zeta)=\frac{w(x_0,y_0,x,y)}{a}\frac{D_0(1-\nu^2)}{\overline{P}a},$$

where a and b are the length and width of the plate, respectively; ρ_0 is the standard mass density, the characteristic equation is obtained from Eq. (6) as

$$\begin{vmatrix}\mathbf{K}_{00}&\mathbf{K}_{01}&\mathbf{K}_{02}&\cdots&\mathbf{K}_{0m}\\ \mathbf{K}_{10}&\mathbf{K}_{11}&\mathbf{K}_{12}&\cdots&\mathbf{K}_{1m}\\ \mathbf{K}_{20}&\mathbf{K}_{21}&\mathbf{K}_{22}&\cdots&\mathbf{K}_{2m}\\ \vdots&\vdots&\vdots&\ddots&\vdots\\ \mathbf{K}_{m0}&\mathbf{K}_{m1}&\mathbf{K}_{m2}&\cdots&\mathbf{K}_{mm}\end{vmatrix}=\mathbf{0}, \tag{7}$$

where

$$\mathbf{K}_{ij}=\beta_{mj}\begin{bmatrix}\beta_{n0}H_{j0}G_{i0j0}-k\delta_{ij}&\beta_{n1}H_{j1}G_{i0j1}&\beta_{n2}H_{j2}G_{i0j2}&\cdots&\beta_{nn}H_{jn}G_{i0jn}\\ \beta_{n0}H_{j0}G_{i1j0}&\beta_{n1}H_{j1}G_{i1j1}-k\delta_{ij}&\beta_{n2}H_{j2}G_{i1j2}&\cdots&\beta_{nn}H_{jn}G_{i1jn}\\ \beta_{n0}H_{j0}G_{i2j0}&\beta_{n1}H_{j1}G_{i2j1}&\beta_{n2}H_{j2}G_{i2j2}-k\delta_{ij}&\cdots&\beta_{nn}H_{jn}G_{i2jn}\\ \vdots&\vdots&\vdots&\ddots&\vdots\\ \beta_{n0}H_{j0}G_{inj0}&\beta_{n1}H_{j1}G_{inj1}&\beta_{n2}H_{j2}G_{inj2}&\cdots&\beta_{nn}H_{jn}G_{injn}-k\delta_{ij}\end{bmatrix}$$

in which $i=0,1,\ldots,m$; $j=0,1,\ldots,n$.

5. Numerical results

To investigate the validity of the proposed method, numerical results are presented for several specific problems and comparisons are made with previously published results. For the plates with variable thickness in one direction, the thickness h changes according to $h=h_0(1+\alpha x/a)$. In all tables and figures, the symbols F, S, and C denote free, simply supported and clamped edges. Four symbols such as CSFS designate the boundary conditions of the plate, the first indicating the conditions at $x=0$, the second at $y=0$, the third at $x=a$ and the fourth at $y=b$. All the convergent values of the frequency parameters are obtained for the plates by using Richardson's extrapolation formula [16]. Some of the results are compared with those reported previously.

5.1. Two-span continuous plates

Fig. 2 shows the plate with two-span partial line supports. In this figure, the symbols a, b, c and d denote the length of the plate, the width of the plate, the length of the line support parallel to x-direction and the length of the line support parallel to y-direction, respectively. In order to examine the accuracy of the approach described, numerical results are carried out for SSSS, SSCS and CSCS square plates with an one-way line support and SSSS, CCCC, CSCS and CSFS rectangular plates with two-way line supports. These plates with full line supports are considered by choosing $c/a = 0, d/b = 1$ and $c/a = 1, d/b = 1$, respectively. The lowest 10 frequency parameters for plates with an one-way support are presented in Table 1. The lowest 4 frequency parameters are presented in Table 2 for plates with two-way supports and aspect ratio $b/a = 0.5, 1.0, 1.5, 2.0$. The results of these plates obtained by Xiang et al. [13] are also shown in the two tables. It can be seen these numerical results agree well.

The next example treated here is the square plates with two-way partial line supports with the partial line support. Three cases of the partial line support $c/a = d/a = 0$, 0.4, 0.8 are considered. The numerical values for the lowest four natural frequency parameter λ of SSSS, CCCC and SSCS plates with partial line supports and with variable thickness ($\alpha = 0.1$, 0.3, 0.5, 0.8) are given in Tables 3–5. From these tables, it can be noted that the frequency parameters increase with the increase of the thickness. The boundary conditions affect the frequency parameters significantly. The nodal patterns of the first four modes of SSSS square plates with $c/a = d/a = 0, 0.4, 0.8$, $\alpha = 0.1, 0.5, 0.8$ are shown in Fig. 3. From Fig. 3, it can be seen that the effects of the changes of the thickness on the nodal patterns are prominent. With the increase of the thickness, the vertical straight line becomes curve line for the plate with $c/a = 0$, the new vertical nodal line will appear in the thinner part of the plate with $c/a = 0.8$ for third and fourth modes.

In order to investigate the effect of the length of the line support on the frequency parameters, the numerical results are presented for SSSS square plate with uniform thickness. The lowest four frequency parameters versus the ratio of the length of line support and the side of the plate are shown in Fig. 4. It can be found the changes of the lowest four frequency parameters with the increase of the ratio c/a are different. When c/a increases from 0 to 0.2, the first, second and third frequency parameters increase, but the fourth frequency parameter keeps constant. When c/a increases from 0.2 to 0.3, all

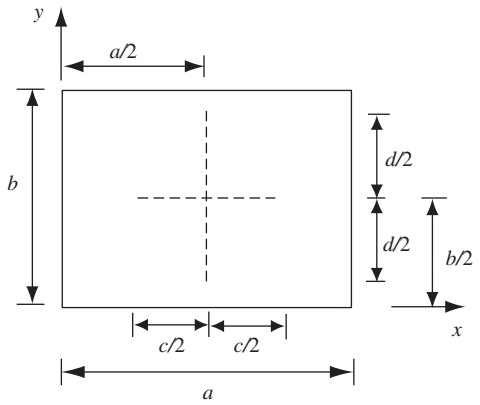

Fig. 2. Rectangular plate with two-way partial line supports.

Table 1
Natural frequency parameter λ for square plates with an one-way full line support ($h/a = 0.01, \alpha = 0.0$).

Mode sequence number	Boundary conditions					
	SSSS		SSCS		CSCS	
	Present	Ref. [13]	Present	Ref. [13]	Present	Ref. [13]
1st	7.19	7.19	7.59	7.60	8.51	8.53
2nd	8.52	8.53	9.34	9.34	9.94	9.96
3rd	9.09	9.10	9.48	9.51	9.96	9.99
4th	9.95	9.96	10.65	10.66	10.99	11.01
5th	11.57	11.60	11.72	11.74	12.09	12.12
6th	12.10	12.12	12.55	12.58	12.77	12.80
7th	13.16	13.26	13.64	13.76	14.62	14.72
8th	14.29	14.39	14.38	14.48	14.73	14.78
9th	14.29	14.39	14.67	14.80	14.93	15.15
10th	14.63	14.72	14.91	15.01	15.50	15.68

Table 2
Natural frequency parameter λ for rectangular plates with two-way full line supports ($h/a = 0.01, \alpha = 0.0$).

B.C	b/a	Ref.	Mode sequence number			
			1st	2nd	3rd	4th
SSSS	0.5	Present	14.36	14.71	17.01	17.21
	1.0	Present	9.09	9.95	9.95	10.64
		Ref. [13]	9.10	9.96	9.96	10.65
	1.5	Present	7.73	8.08	8.90	9.14
	2.0	Present	7.19	7.36	8.52	8.63
CCCC	0.5	Present	17.20	17.48	20.00	20.19
	1.0	Present	10.63	11.53	11.53	12.26
		Ref. [13]	10.65	11.55	11.55	12.29
	1.5	Present	9.13	9.46	10.40	10.63
	2.0	Present	8.62	8.76	10.04	10.14
SSCS	0.5	Present	14.45	14.99	17.06	17.40
	1.0	Present	9.34	10.14	10.65	11.24
		Ref. [13]	9.34	10.15	10.66	11.25
	1.5	Present	8.07	8.39	9.79	9.98
	2.0	Present	7.59	7.74	9.32	9.49
CSFS	0.5	Present	13.16	14.87	15.99	16.18
	1.0	Present	7.13	8.47	10.25	10.89
	1.5	Present	5.32	6.05	9.06	9.14
	2.0	Present	4.53	4.96	7.12	7.75

Table 3
Natural frequency parameter λ for SSSS square plates with two-way partial line supports and variable thickness ($h/a = 0.01, d/a = c/a$).

c/a	α	Ref.	Mode sequence number			
			1st	2nd	3rd	4th
0	0.1	Present	7.36	7.36	7.64	9.31
	0.3	Present	7.64	7.69	8.04	9.73
	0.5	Present	7.89	7.99	8.44	10.13
	0.8	Present	8.23	8.41	8.99	10.70
0.4	0.1	Present	9.31	9.94	9.98	10.38
	0.3	Present	9.64	10.26	10.53	10.97
	0.5	Present	9.92	10.52	11.07	11.57
	0.8	Present	10.30	10.88	11.85	12.42
0.8	0.1	Present	9.31	10.16	10.19	10.94
	0.3	Present	9.65	10.53	10.74	11.52
	0.5	Present	9.95	10.82	11.28	12.13
	0.8	Present	10.34	11.20	12.06	13.01

Table 4
Natural frequency parameter λ for CCCC square plates with two-way partial line supports and variable thickness ($h/a = 0.01, d/a = c/a$).

c/a	α	Ref.	Mode sequence number			
			1st	2nd	3rd	4th
0	0.1	Present	8.96	8.97	9.34	10.89
	0.3	Present	9.27	9.36	9.85	11.38
	0.5	Present	9.53	9.72	10.36	11.83
	0.8	Present	9.88	10.22	11.09	12.47
0.4	0.1	Present	10.87	11.69	11.73	12.31
	0.3	Present	11.26	12.06	12.36	13.01
	0.5	Present	11.58	12.37	13.00	13.71
	0.8	Present	12.00	12.78	13.92	14.71
0.8	0.1	Present	10.87	11.78	11.82	12.57
	0.3	Present	11.27	12.18	12.45	13.27
	0.5	Present	11.59	12.51	13.08	13.96
	0.8	Present	12.02	12.95	14.00	14.96

Table 5
Natural frequency parameter λ for SSCS square plates with two-way partial line supports and variable thickness ($h/a = 0.01, d/a = c/a$).

c/a	α	Ref.	Mode sequence number			
			1st	2nd	3rd	4th
0	0.1	Present	7.47	7.52	8.58	9.72
	0.3	Present	7.75	7.81	9.08	10.15
	0.5	Present	7.96	8.12	9.54	10.56
	0.8	Present	8.27	8.54	10.18	11.12
0.4	0.1	Present	9.45	10.02	10.75	11.20
	0.3	Present	9.72	10.29	10.53	11.41
	0.5	Present	9.98	10.54	12.03	12.57
	0.8	Present	10.33	10.89	11.91	13.49
0.8	0.1	Present	9.49	10.30	10.98	11.60
	0.3	Present	9.77	10.60	11.65	12.30
	0.5	Present	10.03	10.86	12.28	12.97
	0.8	Present	10.39	11.24	13.16	13.90

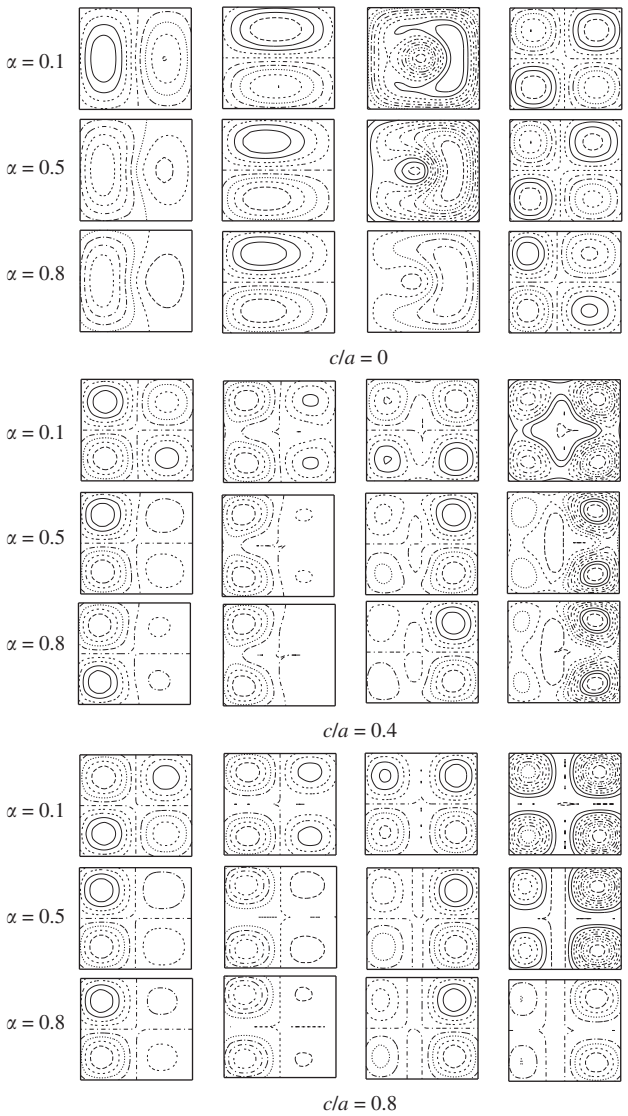

Fig. 3. Nodal patterns for SSSS square plates with two-way partial line supports and variable thickness ($h/a = 0.01, d/a = c/a$).

the frequency parameters increase. When c/a increases from 0.3 to 0.5, the first frequency parameter keeps constant, the second, third and fourth frequency parameters increase. When c/a is larger than 0.5, the frequency parameters almost keep constant. It can also be found that the lowest four frequency parameters are very close for the plate with the ratio $c/a = 0.2$.

5.2. One-way three-span continuous plates

Fig. 5 shows the one-way three-equal-span SSSS rectangular plate continuous over partial line supports parallel to the y-direction. The plate passes over partial line supports at $x = a/3$ and $2a/3$ and has aspect ratio $b/a = 1/3$. The simply supported boundary condition is considered. The lowest four frequency parameters are listed in Table 6 for the plates with

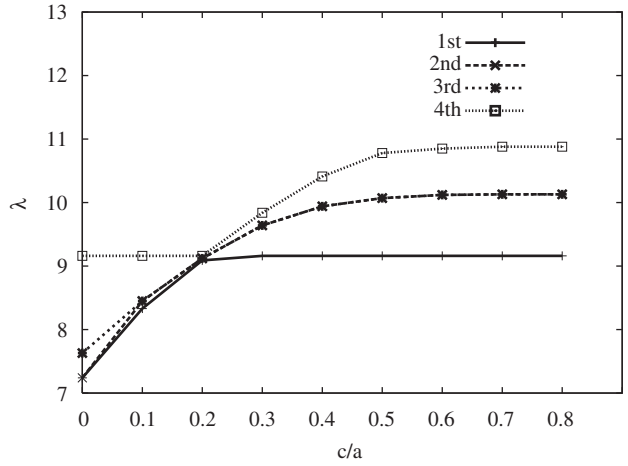

Fig. 4. The frequency parameters versus the ratio c/a of the length of line support and the side of SSSS square plate with two-way partial line supports ($d/a = c/a$).

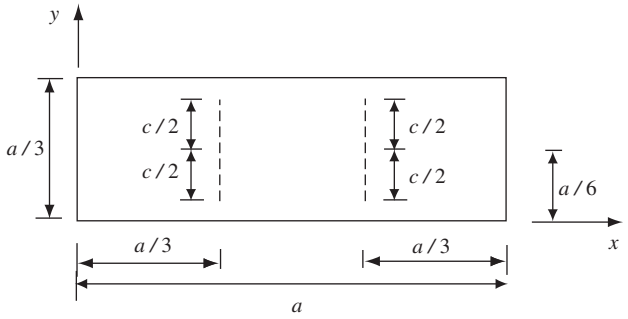

Fig. 5. One-way three-equal-span rectangular plate with partial line supports parallel to the y-direction.

Table 6
Natural frequency parameter λ for one-way three-equal-span SSSS rectangular plates with partial line supports parallel to the y-direction ($h/a = 0.01$).

c/a	α	Ref.	Mode sequence number			
			1st	2nd	3rd	4th
0	0	Present	13.66	14.20	15.30	19.96
	0.1	Present	13.95	14.58	15.69	20.41
	0.5	Present	14.64	16.16	17.31	21.67
1/9	0.0	Present	13.66	14.27	15.58	21.91
	0.1	Present	13.95	14.65	15.98	22.22
	0.5	Present	14.67	16.24	17.59	22.96
1/3	0.0	Present	13.66	14.28	15.60	21.91
		Ref. [3]	13.68	14.31	15.70	21.64
	0.1	Present	13.95	14.66	16.00	22.24
	0.5	Present	14.67	16.25	17.61	22.98

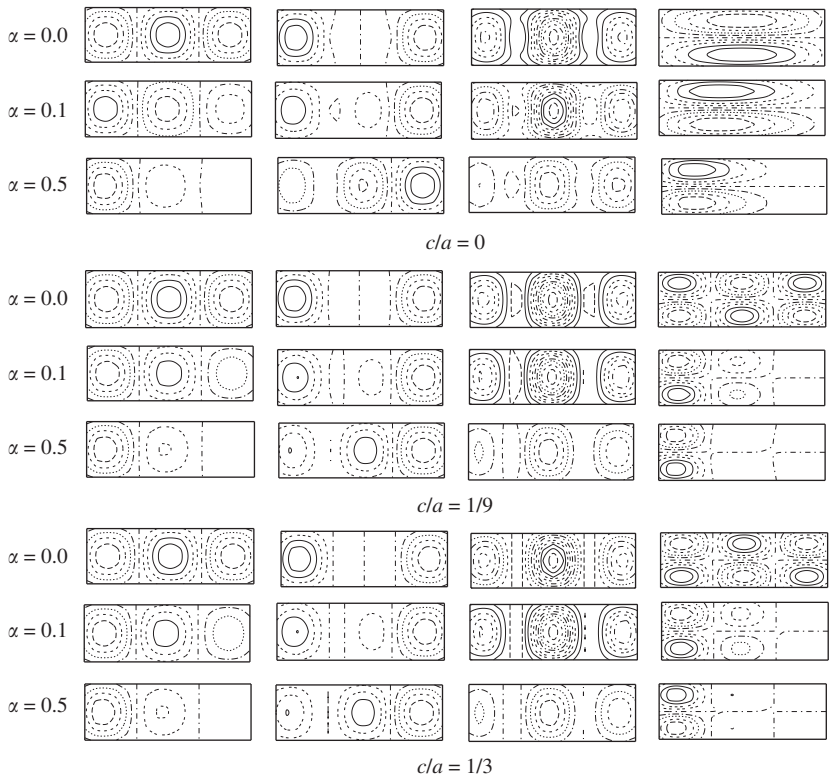

Fig. 6. Nodal patterns for one-way three-equal-span SSSS rectangular plates with partial line support parallel to the *y*-direction.

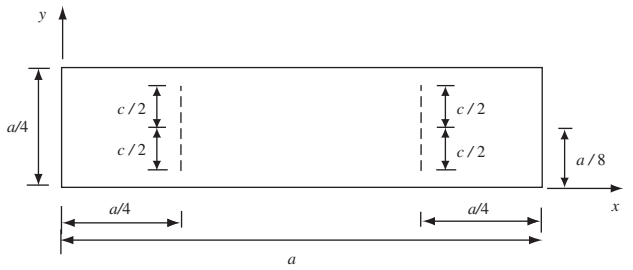

Fig. 7. One-way three-unequal-span SSSS rectangular plate with partial line supports parallel to the *y*-direction.

Table 7
Natural frequency parameter λ for one-way three-unequal-span SSSS rectangular plate with partial line supports parallel to the *y*-direction ($h/a = 0.01$).

c/a	α	Ref.	Mode sequence number			
			1st	2nd	3rd	4th
0	0.0	Present	14.74	18.18	18.86	19.55
	0.5	Present	16.43	19.41	21.00	22.51
	0.8	Present	17.32	19.82	22.26	24.56
1/12	0.0	Present	14.76	18.18	18.95	19.75
	0.5	Present	16.46	19.46	21.12	22.68
	0.8	Present	17.35	19.90	22.38	24.68
1/4	0.0	Present	14.77	18.18	18.96	19.77
		Ref. [3]	14.76	18.25	19.06	19.97
	0.5	Present	16.46	19.47	21.13	22.70
	0.8	Present	17.35	19.91	22.38	24.67

$c/a = 0, 1/9, 1/3$ and variable thickness $\alpha = 0, 0.1, 0.5$. The results obtained by Azimi et al. [3] are also shown in this table. The nodal patterns of the first four modes of these plates are shown in Fig. 6.

Fig. 7 shows the one-way three-unequal-span SSSS rectangular plate with partial line supports parallel to the y-direction. The plate passes over partial line supports at $x = a/4$ and $3a/4$ and has aspect ratio $b/a = 1/4$. The simply supported boundary condition is considered. The lowest four frequency parameters are listed in Table 7 for the plates with $c/a = 0, 1/12, 1/4$ and variable thickness $\alpha = 0, 0.5, 0.8$. The results obtained by Azimi et al. [3] are also shown in this table. The nodal patterns of the first four modes of these plates are shown in Fig. 8. The mode shapes of the plate with $c/a = 1/4$ are very close to the exact mode shapes presented by Azimi et al. [3].

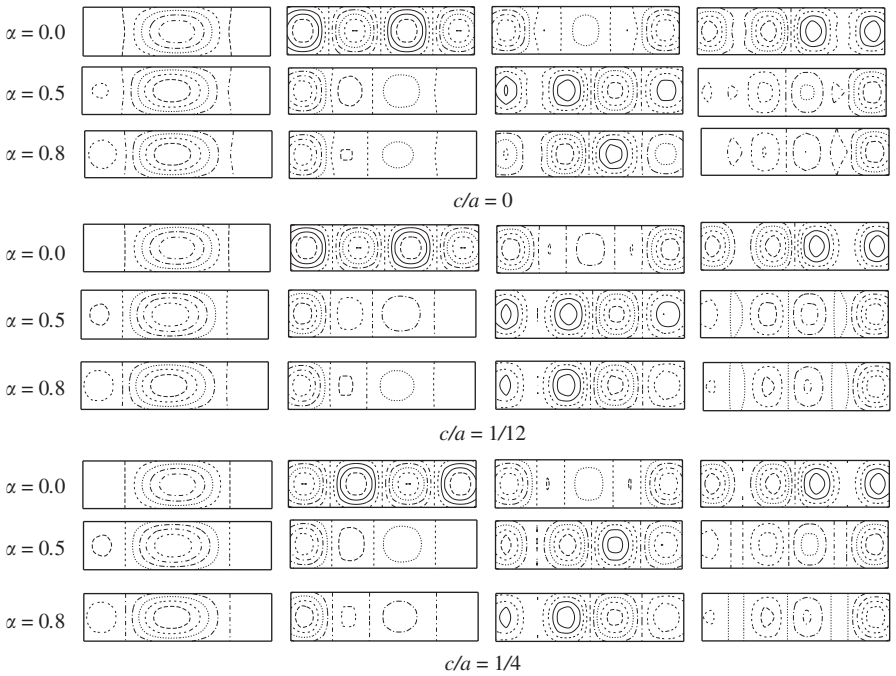

Fig. 8. Nodal patterns for one-way three-unequal-span SSSS rectangular plate with partial line supports parallel to the y-direction.

Table 8
Natural frequency parameter λ for three-ply symmetrically laminated CCCC square plates (0°/90°/0°) with two-span partial line supports and variable thickness ($h/a = 0.01$).

Case	d/a	α	Ref.	Mode sequence number			
				1st	2nd	3rd	4th
One-way	0.5	0.0	Present	19.32	19.76	20.65	21.92
		0.3	Present	20.51	20.94	21.92	23.38
		0.5	Present	21.15	21.55	22.59	23.97
		0.8	Present	21.98	22.35	23.45	24.71
	1.0	0.0	Present	19.32	19.76	20.65	22.40
		0.3	Present	20.51	20.95	21.94	23.71
		0.5	Present	21.16	21.58	22.67	24.31
		0.8	Present	21.98	22.41	23.55	25.16
Two-way	0.5	0.0	Present	19.76	20.02	21.92	22.14
		0.3	Present	20.94	21.26	23.38	23.79
		0.5	Present	21.55	21.93	23.97	24.45
		0.8	Present	22.35	22.77	24.71	25.70
	1.0	0.0	Present	19.76	20.02	22.40	23.16
		0.3	Present	20.95	21.28	23.71	24.71
		0.5	Present	21.58	21.98	24.31	25.73
		0.8	Present	22.41	22.83	25.16	27.17

5.3. Two-span continuous symmetrically laminated plates

At last, natural frequency parameters are given for three-ply symmetrically laminated CCCC square plates (0°/90°/0°) with variable thickness. The following plate parameters are adopted: $E_1/E_2 = 40.0$, $G_{12}/E_2 = 0.6$, $\nu_{12}/E_2 = 0.25$. Here, E_1 is the axial modulus in 1-direction, E_2 is the axial modulus in 2-direction, G_{12} is the shear modulus in 1–2 planes, ν_{12} is the Poisson's ratio associated with loading in the 1-direction and strain in the 2-direction. Some numerical results are given for one-way two-span and two-way two-span plates with partial and full supports by choosing $c/a = 0$ and $d/a = 0.5$, $c/a = 0$ and $d/a = 1$, $c/a = d/a = 0.5$, and $c/a = d/a = 1.0$, as shown in Fig. 3. These numerical results are presented in Table 8.

6. Conclusions

A discrete method is proposed for analyzing the free vibration problem of rectangular plate continuous over full range line supports or partial line supports. No prior assumption of shape of deflection used in the finite element method is employed in this method. Concentrated loads with Heaviside unit functions are used to simulate the line supports. The characteristic equation of the free vibration is obtained by using the Green function. The effects of the line support, the variable thickness and aspect ratio on the frequencies are considered. Some results by the present method have been compared with those previously reported. It shows that the present results have a good convergence and satisfactory accuracy.

Appendix A

$$\mu = b/a; I = \mu(1-\nu^2)(h_0/h)^3; J = 2\mu(1+\nu)(h_0/h)^3; T = ((1+\nu)/5)(h_0/a)^2(h_0/h);$$
$$F_{111} = F_{124} = F_{133} = F_{156} = F_{167} = F_{188} = 1; F_{146} = \nu; F_{212} = F_{223} = F_{235} = F_{247} = F_{266} = \mu;$$
$$F_{257} = \mu\nu; F_{278} = 1; F_{321} = F_{332} = -\mu; F_{345} = F_{354} = -I; F_{363} = -J; F_{372} = -T; F_{377} = 1;$$
$$F_{381} = -\mu T; F_{386} = \mu; \text{other } F_{kts} = 0.$$
$$A_{p1} = \gamma_{p1}, A_{p2} = 0, A_{p3} = \gamma_{p2}, A_{p4} = \gamma_{p3}, A_{p5} = 0,$$
$$A_{p6} = \gamma_{p4} + \nu\gamma_{p5}, A_{p7} = \gamma_{p6}, A_{p8} = \gamma_{p7},$$
$$B_{p1} = 0, B_{p2} = \mu\gamma_{p1}, B_{p3} = \mu\gamma_{p3}, B_{p4} = 0,$$
$$B_{p5} = \mu\gamma_{p2}, B_{p6} = \mu\gamma_{p6}, B_{p7} = \mu(\nu\gamma_{p1} + \gamma_{p5}), B_{p8} = \gamma_{p8},$$
$$C_{p1kl} = \mu(\gamma_{p3} + k_{kl}\gamma_{p7}), C_{p2kl} = \mu\gamma_{p2} + k_{kl}\gamma_{p8},$$
$$C_{p3kl} = J\gamma_{p6}, C_{p4kl} = I_{kl}\gamma_{p4}, C_{p5kl} = I_{kl}\gamma_{p5},$$
$$C_{p6kl} = -\mu\gamma_{p7}, C_{p7kl} = -\gamma_{p8}, C_{p8kl} = 0, [\gamma_{pk}] = [\overline{\gamma}_{pk}]^{-1},$$
$$\overline{\gamma}_{11} = \beta_{ii}, \overline{\gamma}_{12} = \mu\beta_{jj}, \overline{\gamma}_{22} = -\mu\beta_{ij}, \overline{\gamma}_{23} = \beta_{ii}, \overline{\gamma}_{25} = \mu\beta_{jj},$$
$$\overline{\gamma}_{31} = -\mu\beta_{ij}, \overline{\gamma}_{33} = \mu\beta_{jj}, \overline{\gamma}_{34} = \beta_{ii}, \overline{\gamma}_{44} = -I_{ij}\beta_{ij}, \overline{\gamma}_{46} = \beta_{ii},$$
$$\overline{\gamma}_{47} = \mu\nu\beta_{jj}, \overline{\gamma}_{55} = -I_{ij}\beta_{ij}, \overline{\gamma}_{56} = \nu\beta_{ii}, \overline{\gamma}_{57} = \mu\beta_{jj}, \overline{\gamma}_{63} = -J_{ij}\beta_{ii},$$
$$\overline{\gamma}_{66} = \mu\beta_{jj}, \overline{\gamma}_{67} = \beta_{ii}, \overline{\gamma}_{71} = -\mu k_{ij}\beta_{ij}, \overline{\gamma}_{76} = \mu\beta_{ij}, \overline{\gamma}_{78} = \beta_{ii}, \overline{\gamma}_{82} = -H_{ij}\beta_{ij},$$
$$\overline{\gamma}_{87} = \beta_{ij}, \overline{\gamma}_{88} = \beta_{jj}, \text{other } \overline{\gamma}_{pk} = 0, \beta_{ij} = \beta_{ii}\beta_{jj}.$$

Appendix B

$$\overline{a}_{1i0i1} = \overline{a}_{3i0i2} = \overline{a}_{4i0i3} = 1, \quad \overline{a}_{6i0i4} = \overline{a}_{7i0i5} = \overline{a}_{8i0i6} = 1$$
$$\overline{b}_{20jj1} = \overline{b}_{30jj2} = \overline{b}_{50jj3} = 1, \quad \overline{b}_{60jj4} = \overline{b}_{70jj5} = \overline{b}_{80jj6} = 1, \quad \overline{b}_{30002} = 0$$
$$\overline{a}_{pijfd} = \sum_{t=1}^{8}\left\{\sum_{k=0}^{i}\beta_{ik}A_{pt}[\overline{a}_{tk0fd} - \overline{a}_{tkjfd}(1-\delta_{ki})] + \sum_{l=0}^{j}\beta_{jl}B_{pt}[\overline{a}_{t0lfd} - \overline{a}_{tilfd}(1-\delta_{lj})] + \sum_{k=0}^{i}\sum_{l=0}^{j}\beta_{ik}\beta_{jl}C_{ptkl}\overline{a}_{tklfd}(1-\delta_{ki}\delta_{lj})\right\}\overline{b}_{pijgd} = \sum_{t=1}^{8}\left\{\sum_{k=0}^{i}\beta_{ik}A_{pt}[\overline{b}_{tk0gd} - \overline{b}_{tkjgd}(1-\delta_{ki})] + \sum_{l=0}^{j}\beta_{jl}B_{pt}[\overline{b}_{t0lgd} - \overline{b}_{tilgd}(1-\delta_{lj})] + \sum_{k=0}^{i}\sum_{l=0}^{j}\beta_{ik}\beta_{jl}C_{ptkl}\overline{b}_{tklgd}(1-\delta_{ki}\delta_{lj})\right\}$$
$$\overline{q}_{pij} = \sum_{t=1}^{8}\left\{\sum_{k=0}^{i}\beta_{ik}A_{pt}[\overline{q}_{tk0} - \overline{q}_{tkj}(1-\delta_{ki})]\right.$$

$$+\sum_{l=0}^{j}\beta_{jl}B_{pt}[\overline{q}_{t0l}-\overline{q}_{til}(1-\delta_{lj})]+\sum_{k=0}^{i}\sum_{l=0}^{j}\beta_{ik}\beta_{jl}C_{ptkl}-A_{p1}u_{iq}u_{jr}\Bigg\}$$

$$\overline{q}_{1pijcd}=\sum_{e=1}^{8}\Bigg\{\sum_{k=0}^{i}\beta_{ik}A_{pe}[\overline{q}_{1ek0cd}-\overline{q}_{1ekjcd}(1-\delta_{ki})]+\sum_{l=0}^{j}\beta_{jl}B_{pe}[\overline{q}_{1e0lcd}-\overline{q}_{1eilcd}(1-\delta_{lj})]+\sum_{k=0}^{i}\sum_{l=0}^{j}\beta_{ik}\beta_{jl}C_{pekl}\overline{q}_{1eklcd}(1-\delta_{ki}\delta_{lj})\Bigg\}-A_{p1}H_{c}u_{ic}u_{jd}$$

$$\overline{q}_{2pijcd}=\sum_{e=1}^{8}\Bigg\{\sum_{k=0}^{i}\beta_{ik}A_{pe}[\overline{q}_{2ek0cd}-\overline{q}_{2ekjcd}(1-\delta_{ki})]+\sum_{l=0}^{j}\beta_{jl}B_{pe}[\overline{q}_{2e0lcd}-\overline{q}_{2eilcd}(1-\delta_{lj})]+\sum_{k=0}^{i}\sum_{l=0}^{j}\beta_{ik}\beta_{jl}C_{pekl}\overline{q}_{2eklcd}(1-\delta_{ki}\delta_{lj})\Bigg\}-A_{p1}H_{d}u_{ic}u_{id}.$$

References

[1] K. Takahashi, T. Chishaki, Free vibrations of a rectangular plate on oblique supports, *Journal of Sound and Vibration* 60 (1978) 299–304.
[2] K. Takahashi, T. Chishaki, Free vibrations of two-way continuous rectangular plates, *Journal of Sound and Vibration* 62 (1979) 455–459.
[3] S. Azimi, J.F. Hamilton, W. Soedel, The receptance method applied to the free vibration of continuous rectangular plates, *Journal of Sound and Vibration* 93 (1984) 9–29.
[4] C.S. Kim, S.M. Dickinson, The flexural vibration of line supported rectangular plate systems, *Journal of Sound and Vibration* 114 (1987) 129–142.
[5] D. Zhou, K.Y. Cheung, Free vibration of line supported rectangular plates using a set of static beam functions, *Journal of Sound and Vibration* 223 (1999) 231–245.
[6] Y.K. Cheung, J. Kong, The application of a new finite strip to the free vibration of rectangular plates of varying complexity, *Journal of Sound and Vibration* 181 (1995) 341–353.
[7] J. Kong, Y.K. Cheung, Vibration of shear-deformable plates with intermediate line supports: a finite layer approach, *Journal of Sound and Vibration* 184 (1995) 639–649.
[8] Y. Xiang, Y.B. Zhao, G.W. Wei, Levy solutions for vibration of multi-span rectangular plates, *International Journal of Mechanical Science* 44 (2002) 1195–1218.
[9] Y.K. Lin, I.D. Brown, P.C. Deutschle, Free vibration of a finite row of continuous skin-stringer panels, *Journal of Sound and Vibration* 1 (1964) 14–27.
[10] Y. Yong, Y.K. Lin, Free and random vibrations of column-supported cooling towers, *Journal of Sound and Vibration* 98 (1985) 539–563.
[11] D.J. Mead, Y. Yaman, The harmonic response of rectangular sandwich plates with multiple stiffening: a flexural wave analysis, *Journal of Sound and Vibration* 145 (1991) 409–428.
[12] D.J. Mead, Y. Yaman, The harmonic response of uniform beams on multiple linear supports: a flexural wave analysis, *Journal of Sound and Vibration* 141 (1990) 465–484.
[13] Y. Xiang, Y.B. Zhao, G.W. Wei, Discrete singular convolution and its application to the analysis of plates with internal supports—Part 2: applications, *International Journal for Numerical Methods in Engineering* 55 (2002) 947–971.
[14] M. Huang, X.Q. Ma, T. Sakiyama, H. Matsuda, C. Morita, Free vibration analysis of rectangular plates with variable thickness and point supports, *Journal of Sound and Vibration* 300 (2007) 435–452.
[15] S. Timoshenko, S. Woinowsky-Krieger, *Theory of Plates and Shells*, McGraw-Hill, 1959.
[16] Y.S. Fukumoto, Buckling and stable analysis of structures. *Civil Engineers*, 1994.